THE JOURNAL OF BIOLOGICAL CHEMISTRY

Vol. 260, No. 17, Issue of August 15, pp. 9734-9741, 1985
Printed in U.S.A.

^{15}N-labeled *Escherichia coli* tRNA$_f^{Met}$, tRNA^{Glu}, tRNA^{Tyr}, and tRNA^{Phe}

DOUBLE RESONANCE AND TWO-DIMENSIONAL NMR OF N1-LABELED PSEUDOURIDINE*

(Received for publication, March 11, 1985)

Richard H. Griffey‡, Darrell Davis‡, Ziro Yamaizumi§, Susumu Nishimura§, Ad Bax¶, Bruce Hawkins¶, and C. Dale Poulter‡‖

From the ‡Department of Chemistry, University of Utah, Salt Lake City, Utah 84112, the §National Cancer Center Research Institute, Chou-ku, Tokyo, Japan, and ¶National Science Foundation Regional NMR Center, Department of Chemistry, Colorado State University, Fort Collins, Colorado 80523

The N1 imino units in *Escherichia coli* tRNA$_f^{Met}$, tRNA^{Glu}, tRNA^{Phe}, and tRNA^{Tyr} were studied by ^{1}H-^{15}N NMR using three different techniques to suppress signals of protons not attached to ^{15}N. Two of the procedures, Fourier internuclear difference spectroscopy and two-dimensional forbidden echo spectroscopy permitted ^{1}H and ^{15}N chemical shifts to be measured simultaneously at ^{1}H sensitivity. The tRNAs were labeled by fermentation of the uracil auxotroph Sϕ187 on a minimal medium containing [1-^{15}N]uracil. ^{1}H and ^{15}N resonances were detected for all of the N1 Ψ imino units except Ψ13 at the end of the dihydrouridine stem in tRNA^{Glu}. Chemical shifts for imino units in the tRNAs were compared with "intrinsic" values in model systems. The comparisons show that the A·Ψ pairs at the base of the anticodon stem in *E. coli* tRNA^{Phe} and tRNA^{Tyr} have Ψ in an *anti* conformation. The N1 protons of Ψ in other locations, including Ψ32 in the anticodon loop of tRNA^{Phe}, form internal hydrogen bonds to bridging water molecules or 2′-hydroxyl groups in nearby ribose units. These interactions permit Ψ to stabilize the tertiary structure of a tRNA beyond what is provided by the U it replaces.

Pseudouridine (Ψ) is a unique C-nucleoside produced by post-transcriptional modification of selected uridines (U) in the tRNAs of prokaryotes and eukaryotes (1). The base is a highly conserved feature of the TΨC sequence at positions 54–56 and frequently occurs in position 39 at the base of the anticodon stem. Ψ occurs less frequently at other locations. The role of Ψ in tRNAs is not clear. The highly conserved Ψ55 in the TΨC loop occurs at a sharp bend in the phosphodiester backbone and may also bind to ribosomes during protein biosynthesis (2). Ψ39 appears to be an essential feature in tRNAs that participate in regulation of the operon for their cognate amino acids (3, 4). Prominent examples are HisT mutants of *Salmonella typhimurium* which lack the enzyme for conversion of U to Ψ. These strains produce a family of undermodified tRNAs that are charged by their respective aminoacyl synthetases but are defective in regulation (4, 5).

Ψ is potentially considerably more versatile in its hydrogen bonding interactions than the U it replaces. For example, U bonds to A to form a Watson-Crick base pair in a conformation where the pyrimidine carbonyl group adjacent to the glycosidic linkage is *anti* to the ribose ring. An *anti* ΨA Watson-Crick pair of very similar topology can also be formed by using the C2 carbonyl and N3 proton in Ψ to form hydrogen bonds to A (Structure 1). Unlike U, a second structure is possible for Ψ. In this case, the conformation about the glycosidic bond places the C4 carbonyl *syn* to the sugar ring, and the C2 carbonyl and N1 proton interact with A in the base pair. Hurd and Reid (6, 7) noted that an AΨ pair with Ψ in the *anti* orientation resembles a normal Watson-Crick AU pair and suggested that atypical *syn* pairing between A31 and Ψ39 is required for the regulatory function.

Replacement of U by Ψ provides another element of versatility in both the *syn* and *anti* conformations. An "extra" NH moiety is created when the sugar is shifted from N1 in U to C5 in Ψ, and the proton presents a site for formation of a third hydrogen bond to Ψ. An interaction involving the N1 proton should stabilize the structure of the tRNA in the vicinity of Ψ beyond what is possible for U.

When we began this investigation, no reliable techniques existed for determining the conformation of Ψ for AΨ base pairs in tRNAs. The resolution of currently available x-ray structures is too low to distinguish between *syn* and *anti* conformers. Since many of the protons involved in hydrogen bonds in tRNAs exchange slowly with water, they are observed as discreet resonances by NMR spectroscopy. Assignments for the proton attached to N1 of Ψ39 in yeast tRNA^{Phe} based on ^{1}H chemical shifts (6, 7) were, however, unconvinc-

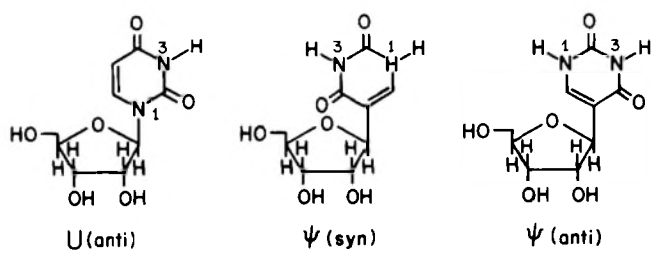

STRUCTURE 1

* This work was supported by Grants GM 32490 from the National Institutes of Health and PCM 79-16861 from the National Science Foundation. Spectra were obtained through the National Science Foundation Regional NMR Center at Colorado State University, funded by National Science Foundation Grant CHE-8208821. The costs of publication of this article were defrayed in part by the payment of page charges. This article must therefore be hereby marked "*advertisement*" in accordance with 18 U.S.C. Section 1734 solely to indicate this fact.

‖ To whom correspondence should be addressed.

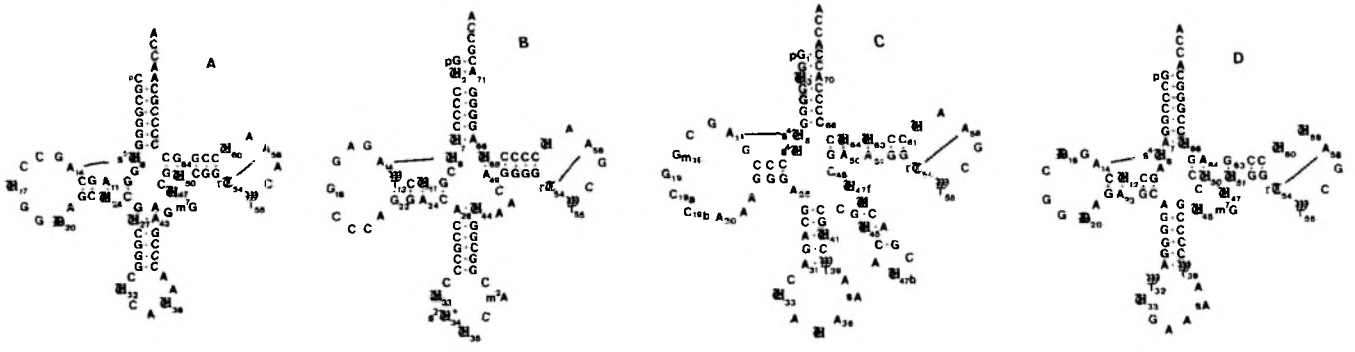

FIG. 1. **Cloverleaf structures of *E. coli* $tRNA_f^{Met}$ (*A*), $tRNA^{Glu}$ (*B*), $tRNA^{Tyr}$ (*C*), and $tRNA^{Phe}$ (*D*).** Labeled bases are indicated with old English letters.

ing. A normally reliable approach based on nuclear Overhauser effects (NOE[1]) (8–10) between protons in Ψ and A also resulted in an incorrect assignment (11). We now report a ^1H-^{15}N NMR study of the pseudouridine N1-H units for the four *Escherichia coli* tRNAs shown in Fig. 1.

EXPERIMENTAL PROCEDURES

Materials—5′-*O*-Acetyl-2′,3′-*O*-isopropylidene adenosine was purchased from Sigma. [1-^{15}N]Uracil was synthesized from potassium [^{15}N]cyanide by the method of Roberts and Poulter (12). A uracil auxotroph of *E. coli* also lacking cytidine deaminase (Sϕ 187) was grown to late log phase at 37 °C on a minimal medium which contained 10 μg/ml of [1-^{15}N]uracil. Crude tRNA was obtained by phenol extraction and isopropyl alcohol precipitation. Pure samples of N1-labeled *E. coli* $tRNA_f^{Met}$, $tRNA^{Glu}$, $tRNA^{Tyr}$, and $tRNA^{Phe}$ were obtained by chromatography on two DEAE-Sephadex columns, the first at pH 7.5 and the second at pH 4.0, according to published procedures (13, 14). The level of incorporation was greater than 90% as determined by the lack of a ^1H peak for unlabeled tRNA between the doublet for the proton at N1 of Ψ55 in $tRNA^{Glu}$.

[1,3-$^{15}N_2$]5-(2′,5′,8′-Trioxadecyl)uracil was prepared from [1,3-$^{15}N_2$]uracil according to the procedures of Cline and co-workers (15). A mixture consisting of 50 mg (0.44 mmol) of [1,3-$^{15}N_2$]uracil (KOR Isotopes), 14.4 mg (0.48 mmol) of paraformaldehyde, and 0.66 ml of 0.5 N potassium hydroxide was allowed to stir for 24 h at 50 °C. The solution was neutralized with 5% hydrochloric acid and water was removed at reduced pressure. The solid residue was dissolved in 7 ml of 2-(2-ethoxyethyl)ethanol, 25 μl of concentrated hydrochloric acid was added, and the resulting solution was allowed to stir at 90 °C for 1 h. Solvent was removed at reduced pressure, and the residue was purified by flash chromatography on silica gel by elution with 85:15 (v/v) chloroform:methanol (R_F = 0.15) to yield 92 mg (80%) of a white solid: ^1H NMR ($CDCl_3$) δ 10.4 (d, 2, H at N1 and N3, $J_{^1H,^{15}N}$ = 95 Hz), 7.78 (s, 1, H6), 4.40 (s, 2), 3.90 (s, 4) 3.80 (s, 4), 3.75 (s, 4), 3.62 (q, 2, J = 6, CH_2 of ethyl), and 1.23 ppm (*t*, 3, J = 6 Hz, CH_3); ^{15}N NMR ($CDCl_3$) 159.0 (N3) and 128.5 ppm (N1).

Tri-*O*-acetyl pseudouridine was synthesized from pseudouridine (Sigma) by the procedure of Bobek and co-workers (16). The material was a colorless glass, R_F = 0.34 on silica gel when eluted with 95:5 (v/v) chloroform:methanol; ^1H NMR ($CDCl_3$) δ 10.38 (br s, 2, H at N1 and N3), 7.72 (s, 1, H at C6), 5.47 (m, 2, H at C1′ and C2′), 4.99 (d, 1, J = 5 Hz, H at C3′), 4.39 (br s, 2), 4.22 (m, 1), and 2.18 ppm (br s, 9, acetyl methyls).

Preparation of NMR Samples—Samples of $tRNA^{Glu}$ (7.0 mg), $tRNA_f^{Met}$ (6.5 mg), and $tRNA^{Phe}$ (8.0 mg) were dissolved in 400 μl of 10 mM cacodylate buffer, pH 7.0, which contained 50 mM sodium chloride, 10 mM magnesium chloride, 1 mM EDTA, and 8% deuterium oxide. $tRNA^{Tyr}$ (6.0 mg) was dissolved in 400 μl of 10 mM cacodylate buffer, pH 7.0, which contained 100 mM sodium chloride, 15 mM magnesium chloride, 1 mM EDTA, and 8% deuterium oxide.

NMR Measurements—^1H and ^{15}N spectra for the model studies were recorded on a Varian FT80-A NMR spectrometer. ^1H chemical shifts were referenced to internal tetramethylsilane or 2,2-dimethyl-2-silapentane-5-sulfonate and ^{15}N chemical shifts, to an external 2.9 M solution of ammonium chloride in 1 M hydrochloric acid. The ^{15}N shifts are given relative to ammonia at 25 °C using a correction factor of 24.9 ppm (17) as previously described (18). NMR data for the tRNAs were obtained on a Nicolet NT 360 MHz spectrometer with a probe triply tuned for ^1H, ^2H, and ^{15}N and an NTC-1180 data processor (19). The 360 MHz ^1H decoupler frequency was mixed down to 36.49 MHz, filtered, amplified, and used for ^{15}N pulses and decoupling. ^{15}N decoupling utilized a WALTZ-16 sequence (20) and the ^{15}N phase variations were controlled by an AdNic Products (Ft. Collins, CO) Black Box.

Three different procedures were used to obtain NMR spectra. Two of the methods, fourier internuclear difference spectroscopy (FINDS) (21, 22) and forbidden echo spectroscopy (FES) (18) yield ^1H and ^{15}N chemical shifts for ^1H-^{15}N units. The third, J-modulated internuclear difference spectroscopy (JIDS), gives ^1H resonances for only those protons bound to ^{15}N. We have previously described applications of FINDS and FES to ^{15}N labeled $tRNA_f^{Met}$ (18, 21). Application of JIDS is described under "Results."

Two-dimensional data sets consisting of 32 blocks of 1600 transients were collected for $tRNA^{Tyr}$ and 48 blocks of 3200 transients were collected for $tRNA_f^{Met}$, $tRNA^{Glu}$, and $tRNA^{Phe}$. The two-dimensional sets were transformed in the t_2 dimension and then "left shifted" in the t_1 dimension by applying a linear phase correction to the two-dimensional data set $S(t_1, F_2)$. After transformation to $S(F_1, F_2)$, the frequencies of the double quantum coherences were plotted as ^{15}N *versus* ^1H chemical shifts.

RESULTS

Detection of Protons in ^1H-^{15}N Pairs—The two most informative procedures for studying ^1H-^{15}N units by NMR are FINDS and FES. Both can be used to obtain ^1H and ^{15}N chemical shifts with the sensitivity of the proton nucleus. The ^1H signals from ^1H-^{15}N units are doublets due to the large internuclear scalar coupling of 90–100 Hz between ^1H and directly bonded ^{15}N. Upon application of a decoupling field at the ^{15}N resonance frequency, the ^1H signal for the attached proton collapses to a single peak while signals for all other protons in the sample do not change. When two free induction decays, one with ^{15}N decoupling on-resonance and the other with ^{15}N decoupling off-resonance, are collected, subtracted, and transformed, the ^1H difference spectrum only shows signals for protons attached to ^{15}N. All other ^1H signals disappear. The resulting FINDS signals appear as 3-line derivative patterns with outer lines (the ^1H-^{15}N doublet) opposite in sign to the inner line (the decoupled ^1H singlet). ^{15}N chemical shifts are obtained by reducing the decoupling power to the minimum needed to collapse the ^1H-^{15}N doublet in a decoupling experiment at a single frequency. A series of ^1H spectra are obtained as the frequency of the ^{15}N decoupler is varied in small increments. The resonance frequency for the nitrogen in an ^1H-^{15}N pair is chosen as the decoupler fre-

[1] The abbreviations used are: NOE, nuclear Overhauser effect; F, frequency dimension; FES, forbidden echo spectroscopy; FINDS, Fourier internuclear difference spectroscopy; INDOR, internuclear double resonance; JIDS, J coupling-modulated internuclear difference spectroscopy; t, time dimension; γ, gyromagnetic ratio.

quency which produces the largest amplitude in the central peak of the FINDS dispersion pattern.

This concept is illustrated by the spectra shown in Fig. 2. Part *B* is a series of ^1H spectra for the imino protons in [1,3-$^{15}N_2$]5-(2′,5′,8′-trioxadecyl)uracil with ^{15}N decoupling at the indicated ^{15}N chemical shifts. Part *A* is a series of the corresponding FINDS spectra. As the frequency of the ^{15}N decoupler is adjusted downfield from 146 ppm, the doublet centered at 13.2 ppm in the ^1H spectrum (the proton at N3) broadens and collapses to a singlet. At the corresponding ^1H chemical shift in the FINDS spectrum, a dispersion pattern appears which reaches maximum intensity for ^{15}N decoupling at 159.9 ppm. The ^1H doublet centered at 11.7 ppm is attached to a nitrogen whose resonance frequency is outside of the range used for ^{15}N decoupling. Hence, this ^1H signal does not change as the ^{15}N decoupler frequency is varied nor does a ^1H signal appear at that position in the FINDS spectrum.

FINDS is the most sensitive of the procedures, and in conjunction with broad band ^{15}N decoupling, can be used to scan for ^1H-^{15}N units. Sensitivity in a FINDS experiment is a function of the separation of the inner peak and the outer peaks since overlap results in a subtraction that reduces intensity. Some losses are experienced for tRNAs where the proton line widths are from 20 to 35 per cent of the ^1H-^{15}N coupling constants. Resolution in the ^1H dimension is a function of the magnitude of the ^1H-^{15}N coupling constant. The line width of a FINDS pattern is equal to the sum of the proton line width plus the ^1H-^{15}N coupling constant. tRNAs typically give FINDS patterns 125 Hz wide, and it is sometimes difficult to disentangle signals for ^1H-^{15}N units whose ^1H and ^{15}N signals are closely spaced. This can limit the accuracy of ^{15}N chemical shifts determined by FINDS. Resolution in the nitrogen dimension is also limited by the level of decoupling power required to collapse the proton doublet, which in some cases may exceed the true nitrogen line width.

Multiple quantum two-dimensional NMR spectroscopy offers several advantages for studying ^1H-^{15}N units. Although not as sensitive as FINDS, the two-dimensional FES experiment is an extraordinarily efficient way to determine ^{15}N chemical shifts. A large range of ^{15}N chemical shifts can be measured in a single experiment, and the resolution is only limited by the true proton and nitrogen line widths. The two-dimensional maps for the four tRNAs required less than 6 h apiece of acquisition time with samples approximately 0.5 mM in ^{15}N. Factors that contribute to the high sensitivity include detection of ^{15}N through the higher γ ^1H nucleus, elimination of ^1H-^{15}N coupling in the ^1H signals, and the short duration of the pulse sequence which avoids excessive loss of magnetization from rapid relaxation of the protons. Additional advantages include the chemical shift dispersion inherent in two-dimensional maps and increased reliability for defining ^{15}N chemical shifts (18).

We have used a third procedure, *J*-modulated internuclear difference spectroscopy (JIDS), to rapidly observe only those protons attached to ^{15}N in a tRNA when nitrogen chemical shift information isn't required. The pulse sequence is shown in Fig. 3. The technique is similar to a classic spin echo experiment with on- and off-resonance 180° pulses on the heteroatom, except the proton 180° pulse is deleted. A selective proton pulse, such as a Redfield 2-1-4 sequence, is used to excite the region of interest without perturbing the large water signal. The spins are allowed to precess for a period $\Delta_1 = 1/2J$. During this time, the protons bonded to ^{12}C and ^{14}N are labeled with the frequency of their chemical shift, while protons bonded to ^{15}N are labeled with both their chemical shift and $\pm\pi J$, depending on the spin state of the nitrogen. When a nitrogen pulse of 180° is applied, the spin state of the nitrogen which the proton sees is interchanged. After an additional time $\Delta_2 = 1/2J$, the *J*-modulated frequency information is lost, and the protons bonded to ^{15}N carry no label from the nitrogen. However, if the 180° pulse is not applied, only the protons attached to ^{15}N continue to dephase by a total of π radians, or 180°, during the evolution period of $2(1/2J)$. When the two experiments are subtracted, the signals from protons bonded to ^{12}C or ^{14}N, which are not frequency modulated by the 180° pulse on ^{15}N, are canceled, and only the signals from protons bonded to ^{15}N remain. The phase error introduced by the effect of the proton chemical shift during the evolution period is resolved by application of a

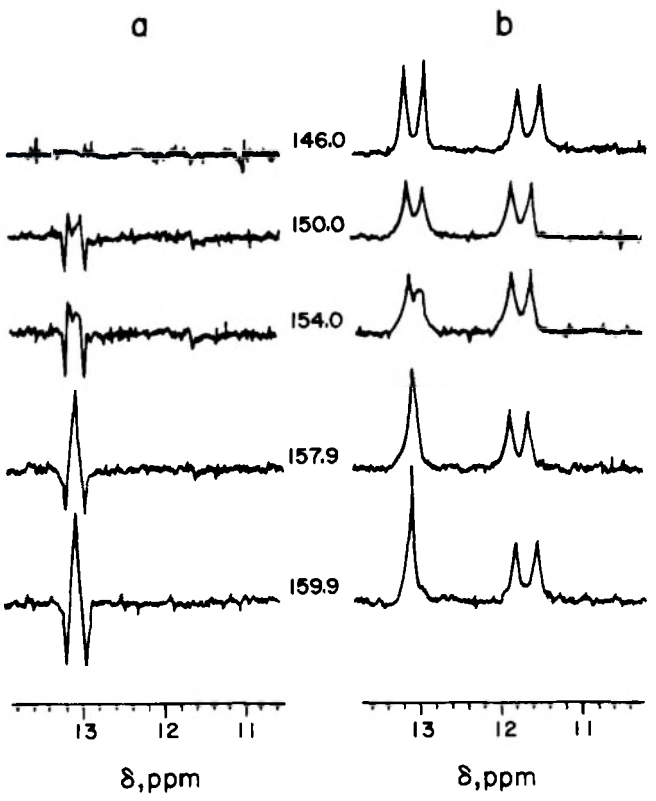

FIG. 2. **Fourier internuclear difference spectroscopy (FINDS) and ^1H spectra of [1,3-$^{15}N_2$]5-(2′,5′,8′-trioxadecyl)uracil.** A 1:1 mixture of [1,3-$^{15}N_2$]5-(2′,5′,8′-trioxadecyl)-uracil and 2′,3′-*O*-isopropylidene-5′-*O*-acetyl adenosine in chloroform-d at 25 °C, 0.2 M total nucleoside concentration. FINDS is shown in part *a* and normal ^1H spectra in part *b*. Sixteen scans were acquired with irradiation of ^{15}N at the chemical shifts indicated between the FINDS and ^1H spectra (on-resonance) or at 1000 Hz downfield from the indicated chemical shift (off resonance).

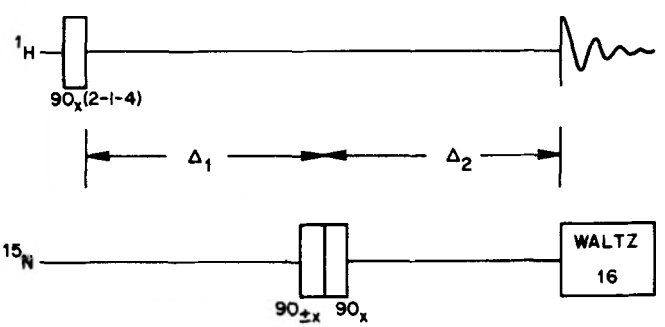

FIG. 3. **Pulse sequence for *J*-modulated internuclear difference spectroscopy.**

first-order phase correction. This procedure gives a simple singlet for each ^1H-^{15}N unit, rather than the broad three-line pattern obtained with difference decoupling at high power. The sequence also avoids the 180° pulse on the protons used in spin echo difference spectroscopy, which is difficult to realize in experiments conducted in H_2O without overloading the dynamic range of the spectrometer. Application of JIDS to *E. coli* $tRNA^{Phe}$ will be presented later in this section.

Model Studies—Formation of hydrogen bonds to the imino protons in nucleic acids is accompanied by downfield shifts in the NMR signals of the proton and the nitrogen. When nucleosides are dissolved in chloroform, the imino protons (23) and nitrogens (24, 25) also experience downfield shifts of similar magnitudes when hydrogen bond acceptors are added to the solution. Model studies with chloroform-soluble derivatives have provided valuable guidelines for assigning NMR peaks of related structures in nucleic acids. Since model shifts were not available for Ψ, we initiated a study to determine the intrinsic and hydrogen bonded chemical shifts for the two imino units in the C-nucleoside. 2′,3′,5′-Tri-*O*-acetyl pseudouridine was used to determine proton chemical shifts, but because ^{15}N labeled Ψ was not available, ^{15}N shifts could only be obtained over a very limited range of concentrations by direct observation on an FT-80A NMR spectrometer. A more complete study was conducted with [1,3-$^{15}N_2$]5-(2′,5′,8′-trioxadecyl)uracil, a chloroform-soluble analog we prepared from [1,3-$^{15}N_2$]uracil.

The ^1H chemical shifts for the protons at N1 and N3 in monomeric Ψ were determined by successive dilution of a chloroform solution of the tri-*O*-acetyl derivative. The signal for the proton at N1 was assigned by its coupling to the proton at C6. Although splitting could not be clearly discerned at ambient temperature, the peak for N1 was broader due to coupling than that for N3. Below 0 °C, the peak for N1 sharpened into a doublet due to the coupling to the proton at C6 (J = 2 Hz). In a 0.2 M chloroform solution of tri-*O*-acetyl pseudouridine at 26 °C, both imino protons resonated at 10.41 ppm. Dilution of the solution disrupted dimer formation and forced the equilibrium population toward the monomeric state. Signals for the protons at N1 and N3 moved upfield to limiting values at infinite dilution of 8.5 and 8.8 ppm, respectively. These chemical shifts are representative of what one might expect when Ψ is located in a hydrophobic pocket. ^{15}N chemical shifts could not be determined at natural abundance with the dilute samples.

Addition of 2′,3′-*O*-isopropylidene-5′-*O*-acetyl adenosine to a solution of tri-*O*-acetyl pseudouridine at 26 °C with total nucleoside concentration maintained at 0.2 M produced a downfield shift in the imino protons at N1 and N3 to limiting values of 11.9 and 13.2 ppm, respectively, as shown in Fig. 4. Both resonances moved further downfield to respective values of 13.17 and 14.17 ppm when the sample was cooled to −35 °C. This behavior is similar to that seen for chloroform-soluble derivatives U or T in the presence of A and suggests that both protons in Ψ form hydrogen bonds to A in the model system. The limiting value of 14.17 ppm for the imino proton at N3 in an AΨ pair is very close to chemical shifts of 14.35 and 14.25 ppm for UA and TA solutions at −35 °C (see Table I). The resonance for the imino proton of G in a GC model is only slightly upfield at 13.93 ppm (25). Chemical shifts in tRNAs vary considerably from measured "intrinsic" values for models because of the anisotropy of neighboring groups. For example, resonances of imino protons in AU pairs have been measured from 12.75 to 14.8 ppm (18), and a similar latitude should be possible for AΨ pairs. It is apparent, therefore, that one cannot distinguish among imino protons

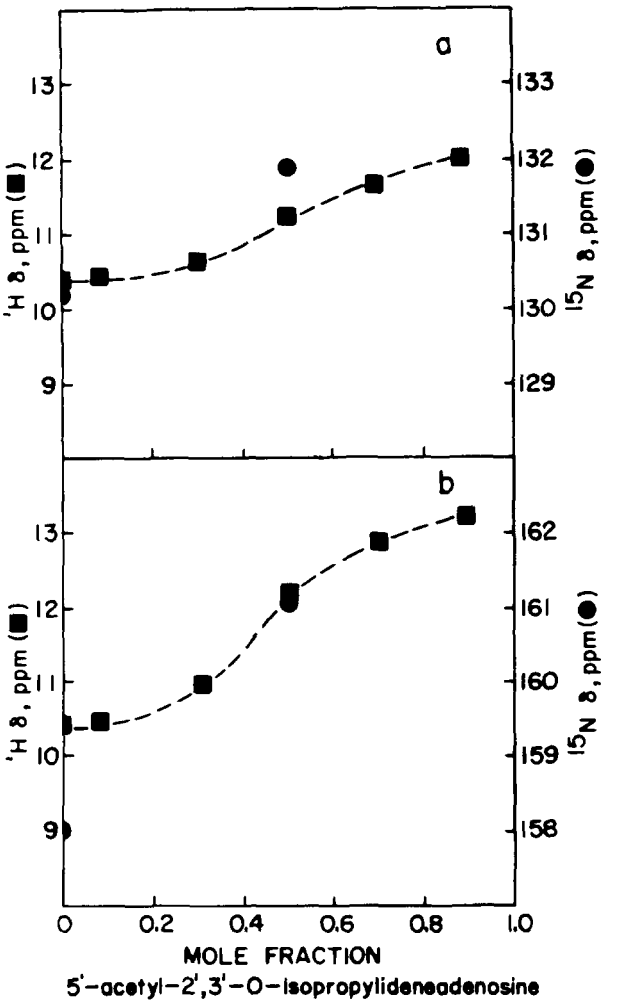

FIG. 4. **^1H and ^{15}N chemical shifts for solutions of 2′,3′,5′-tri-*O*-acetyl pseudouridine and 5′-acetyl-2′,3′-*O*-isopropylidene adenosine.** ^1H chemical shifts (■) were measured with solutions 0.2 M in total nucleoside at 26 °C. ^{15}N chemical shifts (●) were measured with a 1:1 mixture of 0.5 M in total nucleoside at 26 °C. Part *a*, N1 imino unit; part *b*, N3 imino unit.

TABLE I

Model Studies of ^1H and ^{15}N chemical shifts for pyrimidine (Pyr) nucleosides paired with adenosine (A)

Nucleoside	Imino nitrogen	^1H chemical shift		^{15}N chemical shift	
		Pyr	Pyr·A	Pyr	Pyr·A
		δ, ppm		δ, ppm	
2′,3′-*O*-Isopropylidene-5′-*O*-acetyluridine	N3	8.0[a]	14.35[b]	157.3[c]	162.9[b]
2′,3′,5′-Tri-*O*-benzoyl ribothymidine	N3		14.30[b]	155.0[c]	160.4[b]
2′,3′,5-Tri-*O*-acetyl pseudouridine	N1	8.5[d]	13.37[b]	130.2[e]	
	N3	8.8[d]	14.17[b]	158.0[e]	
5-(2′,5′,8′-Trioxadecyl)uracil	N1		12.0[f]	129.0[e]	131.0[f]
	N3		13.3[f]	157.4[e]	161.5[f]

[a] Chloroform solution at 26 °C extrapolated to infinite dilution (26).
[b] Chloroform solution, 0.02 M pyrimidine and 0.18 M 2′,3′-*O*-isopropylidene-5′-*O*-acetyl adenosine at −35 °C.
[c] Chloroform solution, 0.2 M nucleoside at 26 °C.
[d] Chloroform solution extrapolated to infinite dilution at 26 °C.
[e] Chloroform solution, 0.5 M at 26 °C.
[f] Chloroform solution, 0.02 M pyrimidine and 0.18 M 2′,3′-*O*-isopropylidene-5′-*O*-acetyl adenosine at 26 °C.

in AU, AΨ, AT, or GC pairs or between *syn* and *anti* AΨ conformers solely on the basis of proton chemical shifts.

^{15}N chemical shifts were measured for 0.2 M solutions of tri-*O*-acetyl pseudouridine and for solutions 0.1 M in tri-*O*-acetyl pseudouridine and the chloroform-soluble adenosine derivative. The N1 resonance moved downfield from 130.6 to 131.9 ppm, while that for N3 moved from 158.9 to 161.0 ppm. Although we had clearly not attained the concentration of A needed for limiting values, ^{15}N signals could not be measured at lower concentrations of Ψ. These measurements were, however, sufficient to demonstrate the large difference in nitrogen chemical shifts for N1 and N3 and that both resonances are sensitive to the formation of hydrogen bonds.

An analog of Ψ, [1,3-$^{15}N_2$]5-(2′,5′,8′-trioxadecyl)uracil was prepared so the chemical shifts of the pyrimidine nitrogens could be measured over a wider range of concentrations. As shown in Fig. 5, at 26 °C the proton shifts of the N1 and N3 units in the analog moved downfield from 10.2 and 10.4 ppm to 12.0 and 13.3 ppm, respectively, as the mole fraction of adenosine was increased to 0.9. These changes were virtually identical to those observed for tri-*O*-acetyl pseudouridine under similar conditions. In the same sample, shifts for N1 and N3 at 129.0 and 157.4 ppm moved downfield to 131.0 and 161.5 ppm, respectively. Undoubtedly, larger shifts would have occurred at −35 °C. These comparisons of tri-*O*-acetyl Ψ and the analog with uridine in the presence of adenosine are sufficient to demonstrate that one cannot unambiguously distinguish between A·U and A·Ψ pairs by ^1H and ^{15}N chemical shifts when Ψ is in the *anti* conformation. An A·Ψ pair with Ψ in the *syn* conformation, however, should have a H-N1 imino unit with a proton chemical shift near 13 ppm correlated with a unique nitrogen resonance near 132 ppm. The results of the model studies are summarized in Table I.

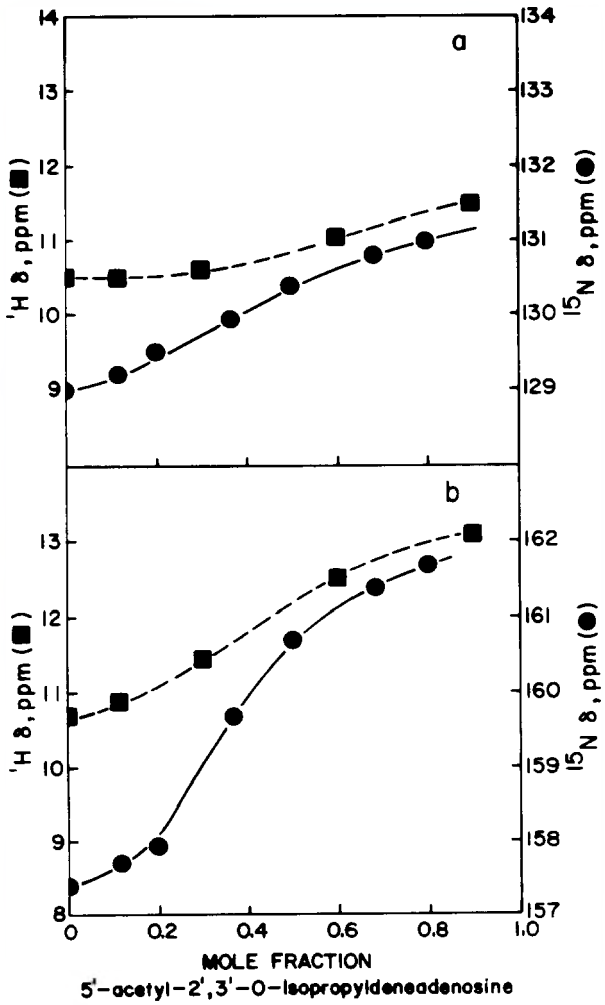

FIG. 5. **^1H and ^{15}N chemical shifts for solutions of [1,3-$^{15}N_2$] 5-(2′,5′,8′)trioxadecyl)uracil and 5′-acetyl-2′,3′-*O*-isopropylidene adenosine.** ^1H (■) and ^{15}N (●) chemical shifts measured with solutions 0.2 M in total nucleoside at 26 °C. Part *a*, N1 imino unit; part *b*, N3 imino unit.

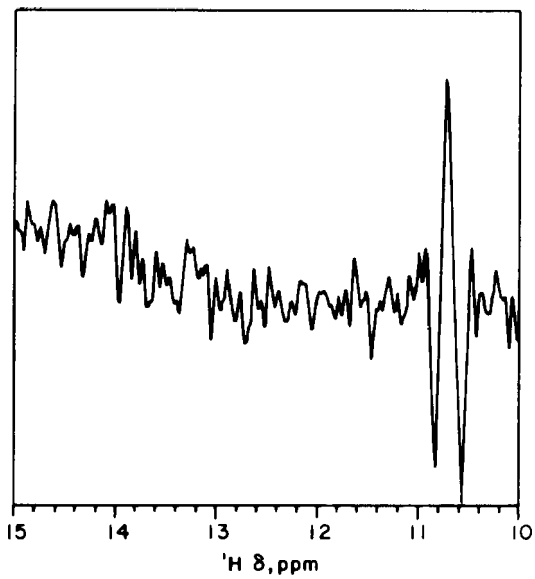

FIG. 6. **A ^1H-^{15}N FINDS spectrum at 15 °C for *E. coli* tRNA$_f^{Met}$.** tRNA$_f^{Met}$ from *E. coli* grown on [1-^{15}N]uracil. The sample was dissolved in 10 mM cacodylate buffer, pH 7.0, containing 50 mM sodium chloride, 10 mM magnesium chloride, 1 mM EDTA, and 8% (v/v) deuterium oxide. A total of 2400 scans was accumulated with broadband irradiation of ^{15}N chemical shift (on-resonance) and 1000-Hz downfield (off-resonance) on alternate scans.

^1H and ^{15}N NMR Spectra of N1 Labeled tRNAs—E. coli tRNA$_f^{Met}$ has a single Ψ at position 55. Correspondingly, a single ^1H peak at 10.57 ppm was observed in the FINDS and FES spectra shown in Figs. 6 and 7. The FINDS spectrum was taken without nitrogen chemical shift correlation, but the FES spectrum gave a correlated nitrogen shift of 134.9 ppm. Clearly, access of the N1 imino proton to bulk solvent is impeded, either by steric exclusion of water or a combination of steric exclusion and hydrogen bonding. The proton and nitrogen chemical shifts are in between values expected for a free N1 unit and one paired with A or a phosphate oxygen.[2] The ^1H shift is in the range expected for Ψ-oxygen interactions when the oxygen donor is a sugar hydroxyl or an immobilized water molecule.

The FES map of tRNA^{Glu} at 15 °C shown in Fig. 8 has a single peak with proton and nitrogen shifts of 10.42 and 135.4 ppm. This resonance is very close to the 10.57 and 134.9 ppm peak for Ψ55 in the two-dimensional map for tRNA$_f^{Met}$ and is assigned to the corresponding base in tRNA^{Glu}. A second peak for Ψ13 is not observed. The small peak seen at 10.5 and 141.0 ppm has a nitrogen shift outside of the known range for N1 units and is attributed to noise. We conclude that the N1 proton in Ψ13 exchanges rapidly with bulk water and a discreet signal is not seen or the resonances for Ψ13 and Ψ55 overlap in both dimensions, a situation not observed for other tRNAs with more than one Ψ.

E. coli tRNA^{Tyr} has Ψ at positions 39 and 55. A FES spectrum of the molecule shows peaks for two ^1H-^{15}N units.

[2] D. R. Davis and C. D. Poulter, unpublished results.

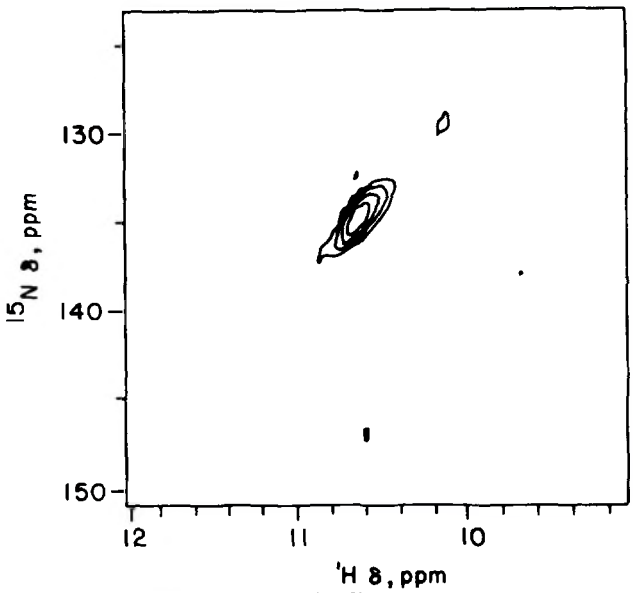

FIG. 7. **A contour map of a ^{1}H-^{15}N FES spectrum at 15 °C for *E. coli* $tRNA_f^{Met}$.** $tRNA_f^{Met}$ from *E. coli* grown on [1-^{15}N]uracil. The sample was prepared as described in the legend to Fig. 5. A total of 1000 × 24 scans was acquired with ^{15}N decoupling. The t_1 dimension was zero-filled to 128 data points and a total of 1000 × 128 points was multiplied by an exponential factor corresponding to 15 Hz of line broadening in each dimension and transformed. The absolute value of the spectrum is plotted.

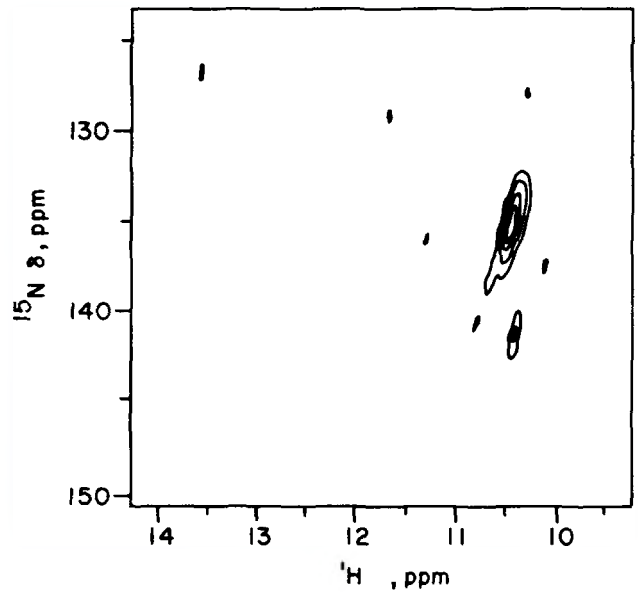

FIG. 8. **A contour map of a ^{1}H-^{15}N FES spectrum at 15 °C for *E. coli* $tRNA^{Glu}$.** $tRNA^{Glu}$ from *E. coli* grown on [1-^{15}N]uracil. The sample was dissolved in 10 mM cacodylate buffer, pH 7.0, containing 100 mM sodium chloride, 15 mM magnesium chloride, 1 mM EDTA, and 8% (v/v) deuterium oxide. A total of 1600 × 20 scans was acquired with ^{15}N decoupling. The t_1 dimension was zero-filled to 128 data points and a total of 2000 × 128 points was multiplied by an exponential factor corresponding to 15 Hz of line broadening in each dimension and transformed. The absolute value spectrum is plotted.

One appears at 10.55 and 135.2 ppm, values nearly identical to those for Ψ55 in $tRNA_f^{Met}$, and we assign this peak to the Ψ55 N1 moiety in $tRNA^{Tyr}$. The other has a proton shift of 10.50 ppm, which overlaps the 10.55 resonance, and a well-resolved nitrogen resonance at 132.4 ppm. Thus, two distinct regions of intensity are seen in the two-dimensional map. The ^{1}H and ^{15}N shifts for the Ψ39 N1 unit are again consistent with hydrogen bonding to a neighboring sugar hydroxyl or an immobilized molecule of water. The ^{1}H chemical shift is clearly outside the range expected for an A·Ψ interaction, demonstrating that Ψ39 does not pair with adenosine in a *syn* A·Ψ Watson-Crick structure under the conditions of the NMR measurement.

E. coli $tRNA^{Phe}$ has pseudouridines located at positions 32, 39, and 55. A JIDS spectrum (see Fig. 9) has ^{1}H peaks at 10.45 and 10.60 ppm with the latter peak having approximately twice the intensity of the former. No ^{1}H signal is observed between 12.5 and 14.0 ppm in the region where the imino proton in an Aψ pair in the *syn* conformation would be expected. The enhanced dispersion provided by ^{1}H-^{15}N chemical shift correlation is nicely illustrated by the FES map shown in Fig. 10 where three well-resolved peaks at 10.45/132.9, 10.60/135.3, and 10.65/132.5 ppm are seen. The two-dimensional resonance at 10.60/135.3 ppm has ^{1}H and ^{15}N shifts which most nearly match those assigned to Ψ55 in $tRNA_f^{Met}$ and $tRNA^{Tyr}$. The tandem shifts to lower field for $tRNA^{Phe}$ indicate a slight change in the environment of the N1 unit, perhaps reflecting a conformation change in the TΨC loop. The peaks at 10.45/132.9, and 10.65/132.5 ppm have chemical shifts similar to that observed for Ψ39 in $tRNA^{Tyr}$ and suggest that the structure of the A31·Ψ39 pair is similar in both tRNAs. One of these two signals must come from Ψ32 in the anticodon loop. Chemical shifts for the tRNAs are summarized in Table II.

DISCUSSION

One of the major limitations of NMR for the study of biopolymers is the high density of peaks in the spectrum. Regions with closely spaced peaks are difficult or impossible to interpret because the resonances cannot be resolved and assigned to specific structural features. This situation is further exacerbated by the broader peaks usually found when studying larger molecules. The power of ^{1}H-^{15}N chemical shift correlation in conjunction with site-specific labeling for circumventing problems associated with spectral density is evident. Of the more than 900 protons and 250 nitrogens in a

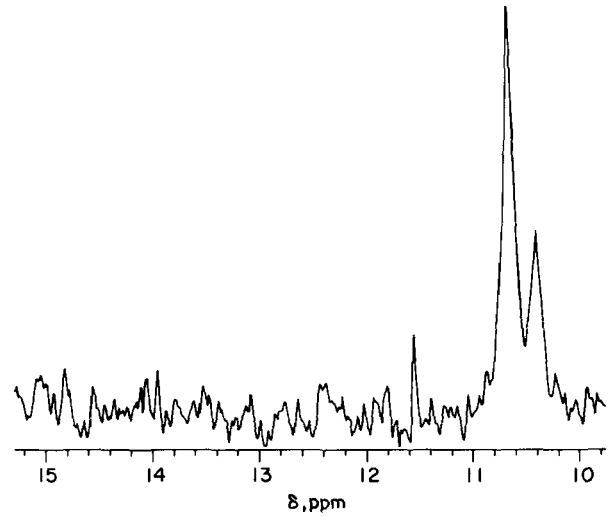

FIG. 9. **A JIDS spectrum at 15 °C for *E. coli* $tRNA^{Phe}$.** $tRNA^{Phe}$ from *E. coli* grown on [1-^{15}N]uracil. The sample was dissolved in 10 mM cacodylate buffer, pH 7.0, containing 50 mM sodium chloride, 10 mM magnesium chloride, 1 mM EDTA, and 8% (v/v) deuterium oxide. A total of 1000 scans was acquired, multiplied by an exponential factor corresponding to 15 Hz of line broadening, and transformed. The absolute value spectrum is plotted.

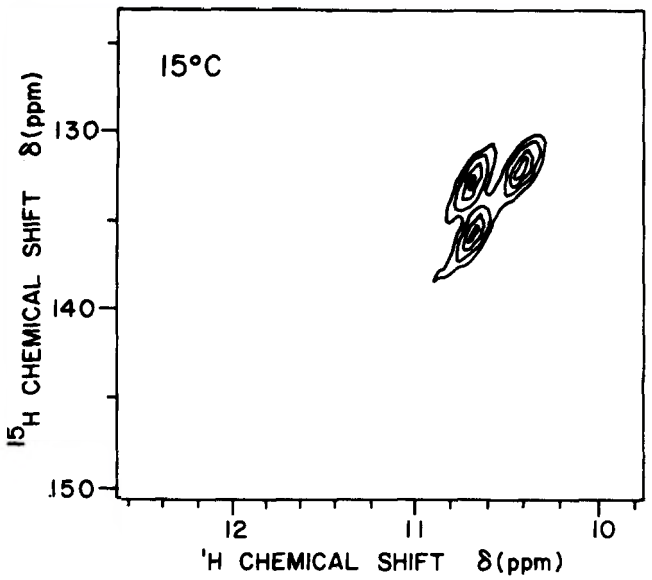

FIG. 10. **A contour map of a ^{1}H-^{15}N FES spectrum at 15 °C for *E. coli* tRNA^{Phe}.** tRNA^{Phe} from *E. coli* grown on [1-^{15}N]uracil. The sample was prepared as described in the legend to Fig. 8. A total of 800 × 24 scans was collected with ^{15}N decoupling. The t_1 dimension was zero-filled to 128 data points, and a total of 2000 × 128 points was multiplied by an exponential factor corresponding to 15 Hz of line broadening in each dimension and transformed. The absolute value spectrum is plotted.

TABLE II

^{1}H and ^{15}N chemical shifts for Ψ N1 imino units in tRNA$_f^{Met}$, tRNA^{Glu}, tRNA^{Tyr}, and tRNA^{Phe} at 15 °C

tRNA	Base	δ ^{1}H[a]	δ ^{15}N[b]
		ppm	
fMet	Ψ55	10.57	134.9
Glu	Ψ13	—[c]	—[c]
	Ψ55	10.42	135.4
Tyr	Ψ39	10.50	132.2
	Ψ55	10.55	134.8
Phe	Ψ32	10.65	132.5
	Ψ39	10.45	132.9
	Ψ55	10.60	135.3

[a] Relative to 2,2-dimethyl-2-silapentane-5-sulfonate.
[b] Relative to NH_3 at 25 °C.
[c] No signal observed.

typical tRNA, the only peaks observed in the spectra of the four tRNAs reported in this study were the N1 imino units of Ψ. There can be no question about the origin of the signals we observed. The tRNAs are labeled with [1-^{15}N]uracil, and of all the bases labeled by uracil, only N1 nitrogens in Ψ have a directly attached proton.

The added dispersion inherent in a two-dimensional FES map or FINDS with ^{15}N chemical shift correlation is essential for resolving peaks in even simple spectra. For example, the two closely spaced Ψ N1 proton resonances in tRNA^{Tyr} resolve nicely in the ^{15}N dimension. The utility of chemical shift correlation is even more impressive for tRNA^{Phe} where the ^{1}H and ^{15}N chemical shifts for Ψ32, Ψ39, and Ψ55 overlap and resolution of the signals depends on the two-dimensional technique. Although the ^{1}H peak at 10.60 is much more intense than the resonance at 10.45 ppm in the JIDS spectrum of tRNA^{Phe}, it would have been hazardous to conclude that two of the three N1 protons have identical shifts. Imino protons in tRNAs often have nonintegral intensities because of difference in rates of relaxation or exchange with solvent (7).

When we began this project there were only a few assignments for Ψ imino protons and no nitrogen measurements in the literature. Tropp and Redfield (27) had attributed a resonance at 10.60 ppm in *E. coli* tRNA$_f^{Met}$ to the imino proton at N1 of Ψ55 on the basis of an elegant experiment in which they observed an NOE from the methyl group in T54. They further proposed that the N1 proton forms a hydrogen bond to a water molecule in the interior of the TΨC loop. We examined this region in the x-ray crystal structure of *E. coli* tRNA$_f^{Met}$ and found two possible interactions (28). One is to a water molecule positioned between the N1 proton and P54, and the other, to the 2′-sugar hydroxyl in T54. Either possibility can be accommodated by a small conformational change in Ψ. Our data do not permit us to distinguish between the two possibilities. Ψ55 is located at a sharp bend in the phosphodiester backbone, and the N1 hydrogen bond may help to stabilize a region under stress.

The conformation of Ψ in A·Ψ pairs has been of interest for several years, especially the A31·Ψ39 interaction found at the base of the anticodon stem in several regulatory tRNAs. Reid and Hurd (6, 7) originally proposed an atypical *syn* structure for the A31·Ψ39 pair in yeast tRNA^{Phe} on the basis of an assignment of the N1 proton resonance to a peak at 13.1 ppm. Roy and co-workers (8, 9) also proposed a *syn* conformation for the pair but recently revised their assignment (11). Their original assignment was based on an NOE from an imino resonance at 13.2 ppm to an aromatic resonance at 6.85 ppm. The signal persisted in a sample deuteriated at the purine C2 position. The most likely candidate for the NOE was the proton at C6 of Ψ, hence the assignment of the 13.2 resonance to the adjacent proton at N1. Unfortunately, deuteration was not complete, and the NOE was apparently to the C2 proton of A31 in residual unlabeled purine. Using a two-dimensional method similar to ours, they now assign the N1 and N3 units in Ψ39 to signals at 10.6/135 ppm and 13.2/163 ppm, respectively. Our results for *E. coli* tRNA^{Phe} and tRNA^{Tyr} clearly support an *anti* A31·Ψ39 pair for these molecules as well. The N1 protons for Ψ39 in the *E. coli* and yeast tRNAs all resonate in the vicinity of 10.5 ppm, a chemical shift consistent with hydrogen bonding of the imino proton to a water molecule or a sugar hydroxyl. The x-ray structure of yeast tRNA^{Phe}, with Ψ39 in the *anti* conformation places N1 approximately 5.5 Å from an oxygen at P38 (29), a distance compatible with hydrogen bonding of the attached proton to a bridging water molecule. There are no nearby sites for a hydrogen bond directly to another part of the tRNA.

Anti A31·Ψ39 pairs in yeast tRNA^{Phe}, *E. coli* tRNA^{Tyr}, and *E. coli* tRNA^{Phe} have topologies very similar to normal A·U pairs. In all cases the proton at N3 is bound to A. Although the locations of C2 and C4 interchange for U and Ψ, the topology of the pyrimidine moiety is similar when viewed from A. The most significant difference between *anti* A·Ψ and A·U pairs is the additional locus for hydrogen bonding present at N1 in Ψ. The small increment in stabilization may be important for reducing conformational mobility in the region of the tRNA which contains Ψ. A·Ψ pairs often are found at the ends of helices where A·U interactions are susceptible to fraying. It should be noted that we failed to detect a resonance for N1 of Ψ13 located at the end of the dihydrouridine stem in *E. coli* tRNA^{Glu}. Perhaps the N1 proton is involved in hydrogen bonding but the interaction is too weak to prevent rapid exchange with water or factors other than stabilization by the N1 proton dictate replacement of U by Ψ at that position.

It is also noteworthy that we saw a resonance for the N1

proton of Ψ32 in the anticodon loop of *E. coli* $tRNA^{Phe}$ with a chemical shift also in the vicinity of 10.5 ppm. As previously discussed for the N1 imino hydrogens in Ψ at other locations, this value indicates hydrogen bonding to a water molecule or a neighboring sugar hydroxyl. Although no x-ray data are available for *E. coli* $tRNA^{Phe}$ an interesting observation can be made using the structure for yeast tRNA. C5 of U32 in yeast $tRNA^{Phe}$ is 5–5.5 Å from oxygens attached at P31 and P32. This position corresponds to the location of N1 if U32 were converted to pseudouridine and changes in overall topology were minimized. The distances are perfect for a hydrogen bond between the N1 proton of Ψ32 and a water molecule bridged to one of the neighboring phosphate oxygens at P31 or P32. Such an interaction would help stabilize the conformation of the anticodon loop. Additional work will be needed to verify this structure for *E. coli* $tRNA^{Phe}$.

^{1}H-^{15}N chemical shift correlation, especially the two-dimensional forbidden echo technique, is a powerful tool for the study of biopolymers in aqueous solutions. The pulse sequence is relatively straightforward and can be performed on most modern high field NMR spectrometers. The sensitivity and resolution of the techniques presented in this paper are inversely proportional to the proton line width for the imino unit, and ultimately the methods will fail for large biopolymers because of excessive broadening of the resonances. We have, however, recently obtained two-dimensional maps of 5 S RNA where the line widths are approximately twice as wide as the 20-Hz lines typically seen for tRNAs. Of course, the proton in any ^{1}H-^{15}N unit must be exchanging slowly with solvent to be observed, which limits detection to bound protons on the surface of a biopolymer or inaccessible protons in the interior of the molecule. Fortunately, the most important protons with respect to structure or catalysis are those which form hydrogen bonds. Although the specific applications discussed in this paper use ^{15}N-labeled tRNAs, the high sensitivity of FINDS and FES make them ideally suited for obtaining ^{15}N spectra of protonated nitrogens at natural abundance when quantities of samples are not limited. Other extensions of the techniques include ^{1}H-^{13}C chemical shift correlation for protonated carbons and metabolic studies with ^{15}N or ^{13}C *in vivo*.

Acknowledgments—We wish to thank Professor Redfield at Brandeis University for a preprint of his work with yeast $tRNA^{Phe}$, Professor Petsko at MIT for permitting us to use his computer graphics facility, Dr. Kanamori at the California Institute of Technology for determining ^{15}N chemical shifts of Ψ, and to Dr. Neuhard at the University of Copenhagen for providing the Sϕ187 strain of *E. coli*.

REFERENCES

1. Goldwasser, E., and Heinrickson, R. L. (1966) *Prog. Nucleic Acid Res. Mol. Biol.* **5,** 399–416
2. Davanloo, P., Sprinzl, M., Watanabe, K., Albani, M., and Kersten, H. (1979) *Nucleic Acids Res.* **6,** 1571–1581
3. Singer, C. E., Smith, G. R., Cortese, R., and Ames, B. N. (1972) *Nat. New Biol.* **238,** 72–74
4. Cortese, R. (1979) in *Biological Regulation and Development* (Goldberger, R. F., ed) Vol. 1, pp. 401–432, Plenum Press, New York
5. Cortese, R., Landsberg, R., Vonder Haar, R. A., Umbarger, H. E., and Ames, B. N. (1974) *Proc. Natl. Acad. Sci. U. S. A.* **71,** 1851–1861
6. Hurd, R. E., and Reid, B. R. (1977) *Nucleic Acids Res.* **4,** 2747–2755
7. Reid, B. R., and Hurd, R. E. (1977) *Accts. Chem. Res.* **10,** 396–402
8. Roy, S., Papastavros, M. Z., and Redfield, A. G. (1982) *Nucleic Acids Res.* **10,** 8341–8349
9. Roy, S., and Redfield, A. G. (1983) *Biochemistry* **22,** 1386–1390
10. Heerschap, A., Haasnoot, C. A. G., and Hilbers, C. W. (1983) *Nucleic Acids Res.* **11,** 4483–4499
11. Roy, S., Papastavros, M. Z., Sanchez, V., and Redfield, A. G. (1984) *Biochemistry* **23,** 4395–4400
12. Roberts, J. L., and Poulter, C. D. (1978) *J. Org. Chem.* **43,** 1547–1550
13. Taya, Y., and Nishimura, S. (1973) *Biochem. Biophys. Res. Commun.* **51,** 1062–1068
14. Vani, B. R., Ramakrishnan, T., Taya, Y., Noguchi, S., Yamaizumi, K., and Nishimura, S. (1979) *J. Bacteriol.* **137,** 1084–1087
15. Cline, R. E., Fink, R. M., and Fink, K. (1959) *J. Am. Chem. Soc.* **81,** 2521–2527
16. Bobek, M., Farkas, J., and Sorm, F. (1969) *Collect. Czech. Chem. Commun.* **34,** 1690–1695
17. Levy, G. C., and Lichter, R. L. (1979) *Nitrogen-15 Nuclear Magnetic Resonance Spectroscopy*, pp. 28–31, Wiley-Interscience, New York
18. Griffey, R. H., Poulter, C. D., Bax, A., Hawkins, B. L., Yamaizumi, Z., and Nishimura, S. (1983) *Proc. Natl. Acad. Sci. U. S. A.* **80,** 5895–5897
19. Bax, A., Griffey, R. H., and Hawkins, B. L. (1983) *J. Magn. Reson.* **55,** 301–315
20. Shaka, A. J., Keeler, J., Frenkiel, T., and Freeman, R. (1983) *J. Magn. Reson.* **52,** 335–338
21. Llinás, M., Horsley, W. J., and Klein, M. P. (1976) *J. Am. Chem. Soc.* **98,** 7554–7558
22. Griffey, R. H., Poulter, C. D., Yamaizumi, Z., Nishimura, S., and Hawkins, B. L. (1983) *J. Am. Chem. Soc.* **105,** 143–145
23. Katz, L., and Penman, S. (1966) *J. Mol. Biol.* **15,** 220–231
24. Poulter, C. D., and Livingston, C. L. (1979) *Tetrahedron Lett.* 755–756
25. Griffey, R. H., and Poulter, C. D. (1983) *Tetrahedron Lett.* 4067–4070
26. Kruger, U., Breuer, H., Abdel Kerim, F. M., Perkampus, H. H., and Scheit, K. H. (1968) *Z. Naturforsch Teil B Anorg. Chem. Org. Chem. Biochem.* **23,** 1360–1366
27. Tropp, J., and Redfield, A. G. (1981) *Biochemistry* **20,** 2133–2140
28. Woo, N. H., Roe, B. A., and Rich, A. (1980) *Nature* **286,** 346–357
29. Kim, S. H., Sussman, J. L., Suddath, F. L., Quigley, G. L., McPherson, A., Wang, A. H. J., Seeman, N. C., and Rich, A. (1974) *Proc. Natl. Acad. Sci. U. S. A.* **71,** 4970–4974